GEOCHEMICAL JOURNAL THE GEOCHEMICAL SOCIETY OF JAPAN

ARTICLE

Distributions of zirconium, niobium, hafnium, and tantalum in the subarctic North Pacific Ocean revisited with a refined analytical method

Ryuta Ueki*, Linjie Zheng, Shotaro Takano, and Yoshiki Sohrin

Institute for Chemical Research, Kyoto University, Uji, Kyoto 611-0011, Japan

* Corresponding author E-mail: ueki.ryuuta.87c@st.kyoto-u.ac.jp

Abstract Although zirconium (Zr), niobium (Nb), hafnium (Hf), and tantalum (Ta) in seawater are potential tracers for water masses, their determination is still a challenge in analytical chemistry. We have refined our preconcentration method using 8-hydroxyquinoline chelating resin (TSK-8HQ) and reinvestigated concentration profiles of the four elements in dissolved (d) and total dissolvable (td) fractions at five different stations from 47 °N, 160 °E to 51 °N, 160 °W in the subarctic North Pacific Ocean. The new method has saved analytical time and reduced systematic errors compared with previous methods. The concentration ranges were 30–276 pmol/kg for dZr, 1.0–2.6 pmol/kg for dNb, 0.09–0.78 pmol/kg for dHf, and 0.006–0.026 pmol/kg for dTa in the subarctic North Pacific Ocean. The concentrations of Zr and Hf increased from surface water to deep water, whereas those of Nb and Ta were nearly constant over the water depth. The profiles of dZr, dNb, and dHf were consistent with those in previous studies. However, we found that dTa is uniformly distributed at 0.015 ± 0.005 pmol/kg (mean ± sd, n = 75), which is approximately one-fifth of that in a previous study. It is likely that the previous dTa data were affected by a systematic error. Negligible differences between td and d fractions suggest that the particulate concentrations of these elements are lower than those reported in a previous study.

Keywords high-field strength elements, seawater, North Pacific Ocean, GEOTRACES

Dates Received: March 30, 2023 Accepted: July 12, 2023 Advance publication: August 1, 2023

Introduction

Zirconium (Zr), niobium (Nb), hafnium (Hf), and tantalum (Ta) are known as high-field strength elements (HFSE) as they form highly charged ions. The dissolved (d) species exist as hydroxide complexes such as $Zr(OH)_5^-$, $Nb(OH)_6^-$, $Hf(OH)_5^-$, and $Ta(OH)_5$ in seawater (Byrne, 2002). The mole ratios of dZr/dHf and dNb/dTa in the Pacific Ocean vary considerably with water masses and are expected to be their tracers (Firdaus *et al.*, 2011). The determination of Zr, Nb, Hf, and Ta in seawater is still a challenge in analytical chemistry. As these elements are not stable in solution without HF, their determination is easily affected by storage conditions and the choice of analytical methods. **Table 1** summarizes the concentrations of dZr, dNb, dHf, and dTa in the open ocean reported previously (Firdaus *et al.*, 2011; Firdaus *et al.*, 2008; Firdaus *et al.*, 2018; Godfrey *et al.*, 1996; Godfrey *et al.*, 2009; McKelvey and Orians, 1993; McKelvey and Orians, 1998; Poehle and Koschinsky, 2017; Rahlf *et al.*, 2021; Rickli *et al.*, 2009; Rickli *et al.*, 2014; Sohrin *et al.*, 1998; Stichel *et al.*, 2012; Sun and Li, 2015; Tanaka *et al.*, 2019). The concentrations of the four elements in seawater are extremely low: 7–380 pmol/kg for dZr, 0.9–30 pmol/kg for dNb, 0.06–3.9 pmol/kg for dHf, and 0.002–7.2 pmol/kg for dTa. In particular, the concentration of Ta in seawater is at least one order of magnitude lower than that of other three elements, which makes the analysis more difficult. The determined maximum concentrations of dTa in the

Citation Ueki, R., Zheng, L., Takano, S. and Sohrin Y. (2023) Distributions of zirconium, niobium, hafnium, and tantalum in the subarctic North Pacific Ocean revisited with a refined analytical method. *Geochem. J.*, **57**, 143–154.

Table 1. Concentration range of dZr, dNb, dHf, and dTa in the open ocean

Site	Zr	Nb	Hf	Ta	References
	[pmol/kg]				
Atlantic Ocean					
47°N–50°N, 14°W–7°W	76–257	—	0.41–2.42	—	Godfrey *et al.* (1996)
22°N–45°N, 38°W–21°W	67–204	—	0.42–1.31	—	Godfrey *et al.* (2009)
56°S–54°N, 63°W–17°E	—	—	0.22–1.50	—	Rickli *et al.* (2009)
59°S–42°S, 64°W–9°E	—	—	0.13–0.70	—	Stichel *et al.* (2012)
12°S–29°N, 48°W–15°W	7–360	1.4–9.6	—	—	Poehle and Koschinsky (2017)
22°N–30°N, 57°W–36°W	18–185	0.9–3.1	0.12–0.52	0.024–0.088	Firdaus *et al.* (2018)
3°S, 0°E	—	—	0.2–1.1	—	Rahlf *et al.* (2021)
Antarctic Ocean					
67°S, 173°W	39–132	1.6–2.9	0.08–0.27	0.019–0.077	Firdaus *et al.* (2011)
66°S–69°S, 27°W–0°E	—	—	0.46–0.75	—	Stichel *et al.* (2012)
72°S–69°S, 164°W–122°W	96–348[a]	—	0.23–1.12[a]	—	Rickli *et al.* (2014)
Indian Ocean					
6°N, 90°E	25–132	1.7–3.2	0.21–0.47	0.024–0.064	Firdaus *et al.* (2018)
Pacific Ocean					
16°N, 168°W	16–295	—	—	—	McKelvey and Orians (1993)
55°N, 145°W	25–366	—	0.20–1.02	—	McKelvey and Orians (1998)
45°N, 165°E	30–250	2.6–4.2	0.10–0.85	0.06–0.29	Sohrin *et al.* (1998)
35°N–51°N, 155°E–165°E	31–275	4.0–7.2	0.14–0.95	0.08–0.29	Firdaus *et al.* (2008)
59°S–50°N, 170°W–160°W	9–249	1.2–3.7	0.06–0.47	0.009–0.118	Firdaus *et al.* (2011)
10°N, 154°W	203–380	15–30	2.2–3.9	4.4–7.2	Sun and Li (2015)
47°N, 160°E	35–269	0.8–3.3	0.12–0.70	0.002–0.028	Tanaka *et al.* (2019)
47°N–51°N, 171°E–160°W	30–276	1.0–2.6	0.09–0.78	0.006–0.026	This study

[a] Unfiltered seawater samples

Pacific varied 280-fold depending on the references.

The preconcentration methods using column extraction with a chelating resin have been reported for the determination of Zr, Nb, Hf, and Ta in seawater. To date we have developed preconcentration methods of the four elements using 8-hydroxyquinoline chelating resin (TSK-8HQ) (Firdaus *et al.*, 2007) and NOBIAS Chelate-PA 1 resin with ethylenediaminetriacetic acid and iminodiacetic acid groups (Tanaka *et al.*, 2019). The vertical profiles of dZr, dNb, dHf, and dTa in the North Pacific were investigated using these methods (Firdaus *et al.*, 2011; Tanaka *et al.*, 2019). The profiles of dZr, dNb, and dHf were similar between the two methods, whereas those of dTa differed by a factor of five. In this study, we refined the TSK-8HQ preconcentration method and analyzed reference materials of seawater and river water. The concentration profiles of the four elements in d and total dissolvable (td) fractions were determined at five stations from 47 °N, 160 °E to 51 °N, 160 °W in the subarctic North Pacific Ocean and compared to those of the previous studies (Firdaus *et al.*, 2011; Tanaka *et al.*, 2019) at cross over stations.

Materials and Methods

Materials and sampling

Deionized water (MQW) made using a Milli-Q Gradient-A-10 system (Merck Millipore, USA) was used to prepare all solutions. Low-density polyethylene (LDPE) bottles (Nalgene, USA) were used for the storage and preparation of all solutions. The bottles were soaked overnight in an alkaline detergent (5% Scat 20-X, Nacalai Tesque, Japan), rinsed with tap water, soaked overnight in 4 mol/kg HCl (reagent grade, FUJIFILM Wako Pure Chemical, Japan), and rinsed using MQW. Then, the bottles were filled with 5 mol/kg HF (Ultrapur-100, Kanto Chemical, Japan), heated to ~80°C in a microwave oven, left overnight, and rinsed thoroughly using MQW. Standard solutions of Zr, Nb, Hf, and Ta were prepared using 1000 mg/kg Inductively Coupled Plasma (ICP) standard solutions (Merck Millipore). We used a high concentration HF solution in a fume hood.

CASS-6 (National Research Council of Canada) is a nearshore seawater reference material for trace metals, which was collected from Halifax Harbour, Canada in October 2014. NASS-7 (National Research Council of

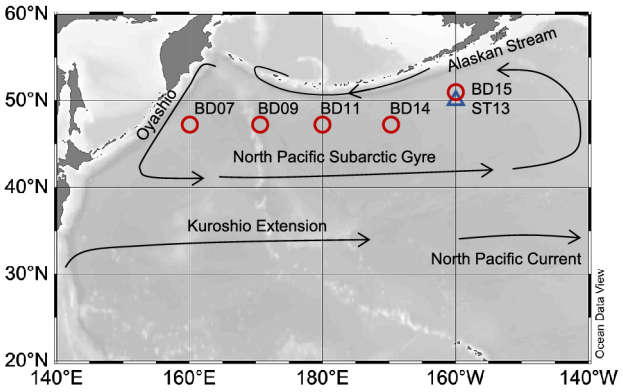

Fig. 1. Map showing the sampling station during the KH12-4 cruise (red circles) and the KH05-2 cruise (blue triangles). The black lines represent surface currents.

Canada) is a seawater reference material for trace metals, which was collected off the continental shelf east of Halifax in August 2014. SLRS-6 (National Research Council of Canada) is a river water reference material for trace metals, which was collected at the City of Ottawa's Britannia Water Purification Plant. JSAC0301-3 (The Japan Society for Analytical Chemistry) is a river water reference material for trace metals, which was collected from the Doshi River, Japan. All the reference materials were added with HF (Ultrapur-100) to the concentration of 2 mmol/kg and stored for more than one month before preconcentration. There are no certificated concentrations of Zr, Nb, Hf, and Ta for the considered reference materials.

Seawater samples were collected from stations BD07, BD09, BD11, BD14, and BD15 (**Fig. 1**) along the GEOTRACES GP02 section (47 °N, 160 °E–129 °W) during the research vessel Hakuho Maru cruise KH-12-4 in August–September 2012. The T-S diagram is shown in Supplementary Fig. 1. The Pacific Deep Water (PDW) was present below 2000 m in depth. At station BD07, the Dichothermal Water (DtW) was observed at approximately 100 m depth. Sampling was conducted using a clean sampling system (Sohrin and Bruland, 2011). HCl (Ultrapur-100, Kanto Chemical) and HF (Ultrapur-100) to concentrations of 10 mmol/kg and 2 mmol/kg, respectively were added to unfiltered samples for total dissolvable metal (tdM) immediately after collection. Samples for dissolved metal (dM) were filtered through an AcroPak capsule filter (pore size: 0.8/0.2 µm) along with the similar immediate addition of HCl and HF. These seawater samples have been stored for about six years until analysis. The difference between tdM and dM concentration was defined as the concentration of labile particulate metal (lpM).

Previously, we reported the vertical profiles of dZr, dNb, dHf, and dTa at stations ST13 (50.005 °N, 159.983 °W) during the KH05-2 cruise in September 2005 (Firdaus *et al.*, 2011) and BD07 (47.000 °N, 160.086 °E) during the KH12-4 in August 2012 (Tanaka *et al.*, 2019). The seawater samples at ST13 were collected using a clean sampling system, filtered with a Nuclepore filter (Pore size: 0.2 µm, Coaster, USA), and analyzed using TSK-8HQ preconcentration method (Firdaus *et al.*, 2007). Filtered seawater samples from BD07 were analyzed using NOBIAS Chelate-PA1 preconcentration method (Tanaka *et al.*, 2019), whereas unfiltered seawater samples from BD07 were analyzed in this study. The stations BD15 and ST13 are regarded as crossover stations because of their proximity. Although the distance between BD09 and BD07 was approximately 796 km, vertical profiles of the four elements are compared at these closest stations in discussion.

Analytical method

We have refined the analytical method using TSK-8HQ for the determination of Zr, Nb, Hf, and Ta in seawater, which was originally developed in our laboratory (Firdaus *et al.*, 2007). Optimization of conditions for preconcentration, elution, evaporation, and redissolution improved robustness of the analytical method. The TSK-8HQ resin was synthesized similarly as in the previous study (Firdaus *et al.*, 2007; Nakagawa *et al.*, 2008). TSK-8HQ was synthesized by mixing 30 g MQW, 3.0 g TOYOPEAL AF-Epoxy-650 (Tosoh Corp., Japan), and 6.0 g 5-amino-8-hydroxyquinoline dihydrochloride (Tokyo Kasei Kogyo, Japan), adjusting the solution pH to 11.5 using 10 mol/kg NaOH (reagent grade, FUJIFILM Wako Pure Chemical), and shaking at 270 r/min, at 60°C, for 12 h using a constant temperature incubator shaker (TAITEC, Japan). The adsorption capacity of TSK-8HQ for molybdenum (Mo) was measured through batch extraction using a solution with 1 mmol/kg Mo at pH = 2, which was 1.07 ± 0.06 mmol/g (mean ± sd, n = 2) being consistent with that of the previous study (Nakagawa *et al.*, 2008).

The TSK-8HQ resin (0.25 g) was packed in a solid-phase extraction cartridge column type L (TOMOE WORKS CO., LTD., Japan; Volume: 0.8 mL) (**Fig. 2**). Two columns connected in series were used for the preconcentration of Zr, Nb, Hf, and Ta. Prior to use, the columns were cleaned using 10 mL of 5 mol/kg HF at a flow rate of 1.0 mL/min and 10 mL of MQW at 2.0 mL/min using a peristaltic pump (MP-3000 EYELA, TOKYO RIKAKIKAI CO., LTD., Japan). The columns were conditioned using 20 mL of 0.02 mol/kg CH_3COOH-NH_3 buffer (pH 5.2 ± 0.2) at 1.0 mL/min. Then, a 250 g seawater sample (pH 5.2 ± 0.2) was passed through the columns at 0.5 mL/min, and 10 mL buffer solution (pH 5.2 ± 0.2) was introduced at 1.0 mL/min to remove the seawater matrix. The analyte metal ions were eluted using 15 mL of 5 mol/kg HF that was flowed at 0.2 mL/min in the opposite direction of the sample loading. The eluate was collected in a LDPE bottle and

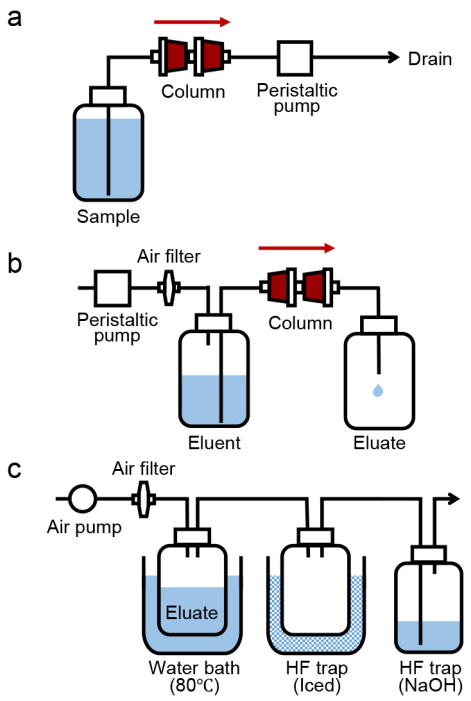

Fig. 2. Schematic diagram of (a) concentration system, (b) elution system, and (c) semi-closed evaporation system.

evaporated to near dryness (~0.1 g solution) in a water bath at 80°C for 4 h, using a semi-closed evaporation system. The residue was redissolved in a 5 g mixture of 2 mmol/kg HF and 0.5 mol/kg HNO_3, shaken at 270 r/min, at 60°C, for 1 h. The exact preconcentration factor was calculated on a weight basis. The concentrations of Zr, Nb, Hf, and Ta in the redissolved solution were determined using a high-resolution ICP mass spectrometer (HR-ICP-MS) Element 2 (Thermo Fisher Scientific, USA) equipped with an Apex HF Desolvating Nebulizer (Elemental Scientific, USA) using a standard curve method. Measured isotopes were ^{90}Zr, ^{93}Nb, ^{178}Hf, and ^{181}Ta.

Results

Verification of analytical method

The procedural blank was determined using MQW as a sample (**Table 2**). The procedural blank for Zr, Nb, Hf, and Ta was similar to that of the previous study (Firdaus *et al.*, 2007; Tanaka *et al.*, 2019). The detection limit was calculated as three times the standard deviation of the procedural blank. For dTa, the procedural blank and detection limit reached 40% of the mean concentration of 0.015 pmol/kg in the open ocean seawater in this study. Thus, further reduction in the procedural blank of Ta is desired in future work. The detection limit of lpM was defined using the following equation considering the propagation of uncertainty: $2 \times \sqrt{2} \times E \times C_{mean}$, where E represents a relative standard deviation (Zr: 0.05, Nb: 0.1, Hf: 0.1, Ta: 0.2) and C_{mean} represents the mean concentration of dM in this study (Zheng *et al.*, 2019).

Table 2. Procedural blank and detection limit

Metal	Unit	Fraction	Procedural blank		Detection limit
			n	mean	
Zr	pmol/kg	td	11	1.6	4.3
		d	30	2.0	2.6
		lp	—	—	22
Nb	pmol/kg	td	11	0.16	0.12
		d	30	0.05	0.10
		lp	—	—	0.56
Hf	pmol/kg	td	11	0.02	0.06
		d	30	0.03	0.05
		lp	—	—	0.12
Ta	pmol/kg	td	11	0.007	0.004
		d	30	0.006	0.006
		lp	—	—	0.009

Seawater samples that were collected from different depths in the Pacific Ocean were mixed to prepare two aliquots of mixed seawater for the recovery experiments of Zr, Nb, Hf, and Ta. The mixed seawater was spiked with known concentrations (addition of 0.05–300 pmol/kg) of the four elements from pure standards. The recoveries were calculated from the difference between spiked and unspiked seawater samples. The mean recovery of Zr, Nb, Hf, and Ta was 95–101%, 99–101%, 97–102%, and 100–107%, respectively (**Table 3**). The standard deviation was less than 8%. These results indicate that our method can preconcentrate the four elements quantitatively. Elemental concentrations were reproducible within 10% for Zr, Nb, and Hf and 20% for Ta (based on 2 sd against the mean). In addition, the volume of eluent was 15 mL in this method and 60 mL in the NOBIAS Chelate-PA1 method. As a result, the amount of reagent, elution time, and evaporation time could be saved by using the TSK-8HQ method.

Analysis of natural water reference materials

Table 4 summarizes the concentrations of dZr, dNb, dHf, and dTa in natural water reference materials used in this study and some previous studies (Babechuk *et al.*, 2020; Bayon *et al.*, 2011; Firdaus *et al.*, 2008; Firdaus *et al.*, 2007; Poehle *et al.*, 2015; Raso *et al.*, 2013; Sasmaz *et al.*, 2021; Sun and Li, 2015; Tanaka *et al.*, 2019; Yeghicheyan *et al.*, 2019). The concentrations of dZr, dNb, dHf, and dTa in CASS-6, NASS-7, and JSAC0301-3 are reported for the first time in this study. The concentrations of dZr, dNb, and dHf in CASS-6 were within the concentration ranges of CASS-3, 4, and 5. The concentration of dTa in CASS-6 was close to that in CASS-5 reported in previous study (Tanaka *et al.*,

Table 3. Recovery from mixed seawater

Mixed seawater #1			
Metal	Concentration [pmol/kg][a]		Recovery [%][a]
	Added	Found	
Zr	0	78.2 ± 1.7	
	232 ± 4	314 ± 7	101 ± 4
Nb	0	3.11 ± 0.20	
	2.33 ± 0.04	5.44 ± 0.13	99 ± 5
Hf	0	0.34 ± 0.01	
	0.73 ± 0.01	1.09 ± 0.01	102 ± 2
Ta	0	0.046 ± 0.007	
	0.056 ± 0.001	0.103 ± 0.004	100 ± 8

[a] mean ± sd for four replicates

Mixed seawater #2			
Metal	Concentration [pmol/kg][b]		Recovery [%][b]
	Added	Found	
Zr	0	72.1 ± 3.2	
	156 ± 2	230 ± 2	101 ± 3
	302 ± 6	361 ± 3	95 ± 2
Nb	0	2.50 ± 0.15	
	2.81 ± 0.04	5.34 ± 0.15	101 ± 4
	5.42 ± 0.11	7.95 ± 0.03	99 ± 1
Hf	0	0.41 ± 0.03	
	0.65 ± 0.01	1.01 ± 0.01	101 ± 4
	1.26 ± 0.03	1.66 ± 0.04	97 ± 2
Ta	0	0.041 ± 0.002	
	0.073 ± 0.001	0.116 ± 0.002	103 ± 3
	0.141 ± 0.003	0.194 ± 0.003	107 ± 2

[b] mean ± sd for three replicates

2019). The observed concentrations of dZr, dNb, and dHf in NASS-7 were within the concentration ranges of NASS-5 and 6. The concentration of dTa in NASS-7 was close to that in NASS-6 reported in previous study (Tanaka *et al.*, 2019).

In river water, there were considerable variations in the concentrations of four elements in SLRS-6. The concentrations of dZr and dHf in SLRS-6 of this study are similar to those reported for SLRS-4 (Bayon *et al.*, 2011). The dNb concentration in SLRS-6 observed in this study was close to that reported for SLRS-3 (Firdaus *et al.*, 2008). The dTa concentration in SLRS-6 observed in this study was in a range of concentrations reported for SLRS-3 and 6 (Babechuk *et al.*, 2020; Firdaus *et al.*, 2008). We found that the concentrations in Japanese river water (JSAC0301-3) were 3–7% of those in the Ottawa River water.

HF was added to natural water reference materials at 2 mmol/kg and stored for more than one month before preconcentration. To check the adsorption of four elements on the wall of LDPE bottles of the reference materials, empty bottles were rinsed with 15 mL 5 mol/kg HF by shaking at 270 r/min, at 60°C, for 6 h. Then the metal concentrations in the HF solution were determined. The adsorption percentage of Zr, Nb, and Hf was less than 5% of the total amount, while that of Ta was 26 ± 9% (n = 6, Supplementary Table 1). The results were consistent with previous study (Tanaka *et al.*, 2019) and suggested that dTa was adsorbed on the wall of reference material bottles before addition of HF. When 2 mM HF was added immediately after sampling, the adsorption percentage of Ta was less than 10% at least for about six years.

Distributions of Zr, Nb, Hf, and Ta in the subarctic North Pacific Ocean

Figure 3 shows the vertical profiles of dZr, dNb, dHf, and dTa at stations BD09, BD11, BD14, and BD15. **Figure 4** shows full-depth sectional distributions of dZr, dNb, dHf, and dTa from 47 °N, 171 °E to 51 °N, 160 °W. The vertical profiles of each element were similar among the four stations within a relative standard deviation. Dissolved Zr concentration increased from 30 pmol/kg in surface water to 276 pmol/kg in deep water. Dissolved Hf concentration increased from 0.09 pmol/kg in surface water to 0.78 pmol/kg in deep water. Dissolved Nb concentration was 1.8 ± 0.2 pmol/kg (n = 44) in surface water (<1000 m) and slightly increased to 2.2 ± 0.2 pmol/kg (n = 40) in deep water (>1000 m). Mean concentration of dTa was 0.015 ± 0.005 pmol/kg (n = 75) without any obvious trend with depth. Supplementary Fig. 2 shows the full-depth sectional distributions of tdZr, tdNb, tdHf, and tdTa at stations BD07, BD09, BD11, BD14, and BD15. Supplementary Fig. 3 shows the profiles of tdM/dM ratio of each element, and the dM concentrations at BD07 were cited from the previous study (Tanaka *et al.*, 2019). The mean ratio was 0.99 ± 0.09 (n = 102) for tdZr/dZr, 1.02 ± 0.18 (n = 103) for tdNb/dNb, 0.95 ± 0.19 (n = 89) for tdHf/dHf, and 0.96 ± 0.40 (n = 89) for tdTa/dTa. These results suggested that the concentrations of tdZr, tdNb, tdHf, and tdTa were almost similar to those of dZr, dNb, dHf, and dTa. The lpMs were detected for less than 5% of all the samples. Particularly, lpZr, lpNb, lpHf, and lpTa were detected in the bottom water of BD15 (depth: 4853 m).

Discussion

Comparison of the concentrations of dZr, dNb, dHf, and dTa at crossover stations

The results of the procedural blank, detection limit, and analysis of reference materials suggested that the proposed method has sufficient accuracy and precision for

Table 4. Concentrations (mean ± sd) of dZr, dNb, dHf, and dTa in natural water reference materials

Sample	*n*	Zr	Nb	Hf	Ta	Notes
		[pmol/kg]				
Seawater						
CASS-3	1	90	6.7	0.49	0.21	Firdaus *et al.* (2008)
CASS-4	3	271 ± 4	—	1.9 ± 0.2	—	Bayon *et al.* (2011)
CASS-5	9	407 ± 69	20 ± 6	5 ± 1	11 ± 7	Sun and Li (2015)
	2	218 ± 6	4.0 ± 0.3	1.49 ± 0.04	0.022 ± 0.002	Tanaka *et al.* (2019)
CASS-6	2	280 ± 3	5.2 ± 0.04	1.67 ± 0.02	0.022 ± 0.001	This study
NASS-5	2	183 ± 9	7.8 ± 0.9	1.2 ± 0.2	0.25 ± 0.15	Firdaus *et al.* (2007)
	5	165 ± 10	—	0.9 ± 0.1	—	Bayon *et al.* (2011)
NASS-6	3	246 ± 32	—	4.9 ± 0.5	—	Raso *et al.* (2013)
	1	105	3.0	—	—	Poehle *et al.* (2015)
	9	384 ± 66	27 ± 11	4 ± 1	11 ± 6	Sun and Li (2015)
	2	247 ± 6	4.2 ± 0.2	1.68 ± 0.05	0.023 ± 0.001	Tanaka *et al.* (2019)
	5	260 ± 6	—	2.9 ± 1.5	—	Sasmaz *et al.* (2021)
NASS-7	2	242 ± 3	6.5 ± 0.3	1.23 ± 0.03	0.027 ± 0.002	This study
River water						
SLRS-3	1	678	31	4.9	1.4	Firdaus *et al.* (2008)
SLRS-4	3	1021 ± 33	—	16.9 ± 0.2	—	Bayon *et al.* (2011)
SLRS-6	1	681	87	53	—	Yeghicheyan *et al.* (2019)
	1	722	28	11.2	0.33	Babechuk *et al.* (2020)
	2	1078 ± 26	30.5 ± 0.9	14.4 ± 0.9	0.52 ± 0.03	This study
JSAC0301-3	2	37 ± 1	2.2 ± 0.1	0.44 ± 0.01	0.026 ± 0.002	This study

the marine geochemical study of Zr, Nb, Hf, and Ta. The comparison of vertical profiles at stations located at the same position and occupied during different cruises (crossover stations) is useful to investigate the quality of oceanographic data.

The vertical profiles of dZr, dNb, dHf, and dTa in this study (BD09 and BD15) were compared to those of the previous studies (BD07 and ST13). The vertical profiles of dZr were similar among the four stations, while those of dNb, dHf, and dTa at ST13 showed the largest difference from those at the other three stations (**Fig. 5**). For dZr, the data at BD15 against ST13 showed strong linearity with a regression line of slope (0.95), indicating both the data are consistent (Supplementary Fig. 4). The dHf data also showed a strong correlation with a slope of 1.27. However, the correlation was poor for dNb and dTa. Although BD09 and BD07 were not necessarily crossover stations, the regression lines for dZr and dHf were close to the 1:1 line, indicating they were consistent between the two stations (Supplementary Fig. 5). The correlation is not strong for dNb and dTa. This is partly because the concentrations of dNb and dTa were almost uniform across the water depth. As an alternative, mean concentrations of dNb and dTa were compared among different stations (Supplementary Table 2). The mean concentrations of dNb and dTa indicated consistency between BD09 and BD07.

In conclusion, our new data are consistent with those reported in our previous paper (Tanaka *et al.*, 2019), although different chelating resins were used. Previous studies (Firdaus *et al.*, 2011; Firdaus *et al.*, 2008) were potentially affected by systematic errors. Particularly, the dTa concentrations in the previous study (Firdaus *et al.*, 2011) were five times higher than those in this study. Although many reported concentration values of dZr, dNb, dHf, and dTa in CASS and NASS are inconsistent, the data from this study and Tanaka *et al.* (2019) exhibit comparable results (**Table 4**). In contrast, dTa concentration by Firdaus *et al.* (2007) is higher by one order of magnitude than that by Tanaka *et al.* (2019) and this study. These results suggest that there were systematic errors in Firdaus *et al.* (2007), which resulted in higher dTa concentration in ocean data.

Although the exact reason for the systematic error cannot be identified, a few possible reasons include (1) contamination during filtration. The filtration using Nuclepore filters in the previous study may have caused higher contamination than that using AcroPaK capsule filters. In the case of the determination of dissolved lead in seawater, a significantly high blank was detected in

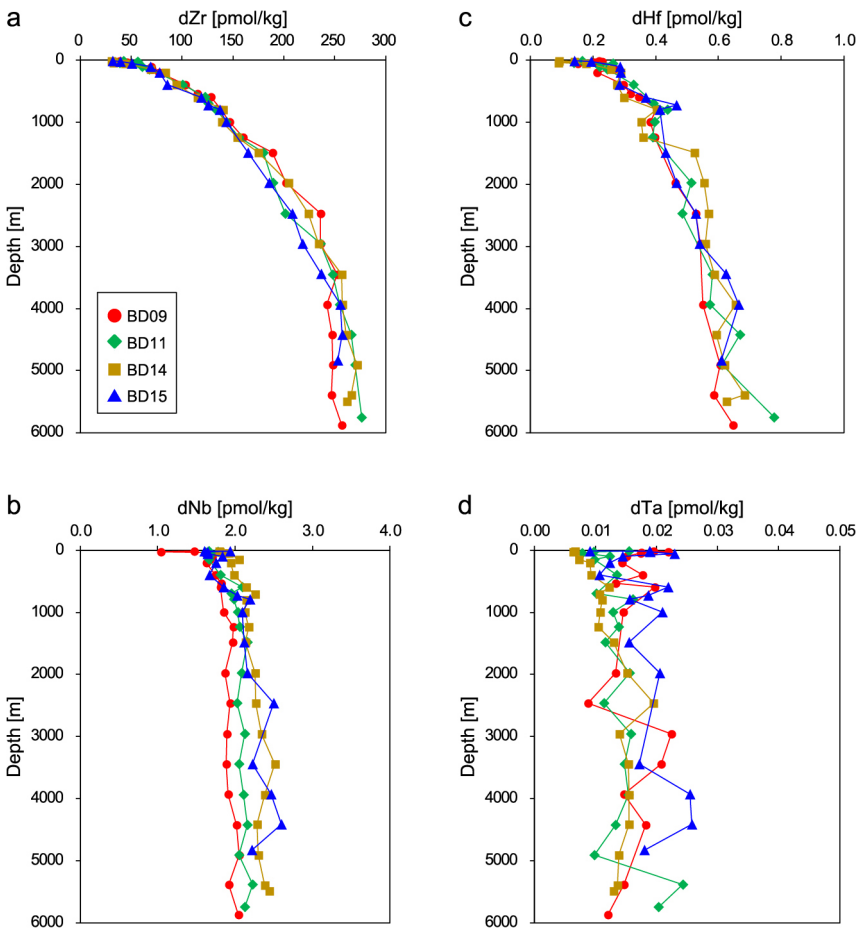

Fig. 3. Vertical profiles of (a) dZr, (b) dNb, (c) dHf, and (d) dTa at stations BD09 (red circles; 47.000 °N, 170.583 °E), BD11 (green diamonds; 47.002 °N, 179.995 °E), BD14 (yellow squares; 47.000 °N, 169.998 °W), and BD15 (blue triangles; 50.834 °N, 160.000 °W).

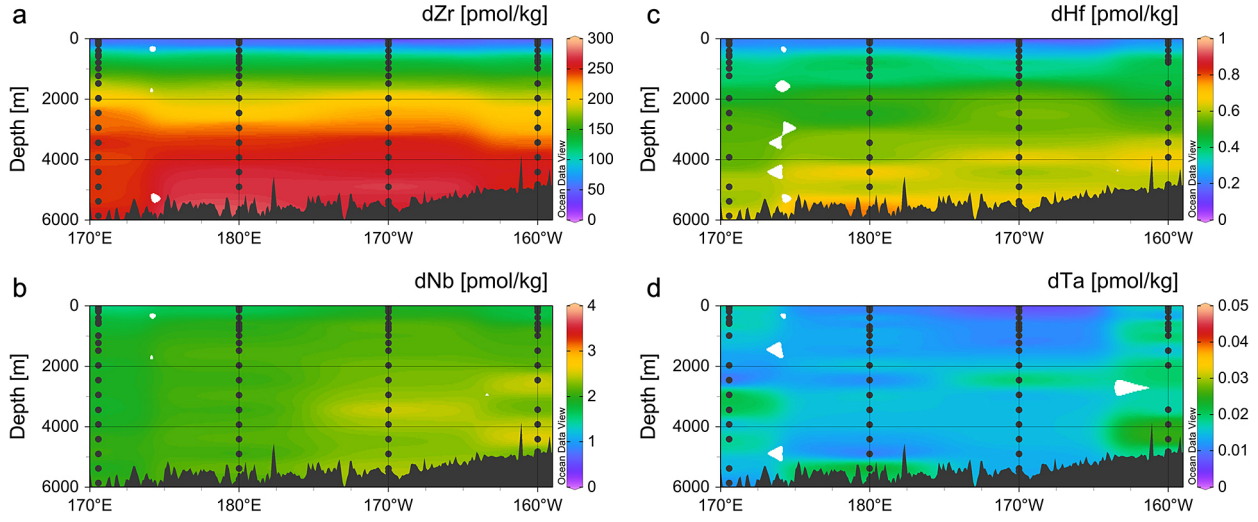

Fig. 4. Full-depth sectional distributions of (a) dZr, (b) dNb, (c) dHf, and (d) dTa from 47 °N, 171 °E to 51 °N, 160 °W.

MQW filtered with Nuclepore filters (Zheng *et al.*, 2019), (2) error in calibration using standard solutions. The standard solutions in this study and the last study (Tanaka *et al.*, 2019) were prepared in 1–2 mmol/kg HF and 0.5 mol/kg HNO_3. However, the standard solutions in the previous study (Firdaus *et al.*, 2011) were prepared in 1 mol/kg HNO_3, which did not contain HF. We have observed adsorption of Ta on the bottle of the reference

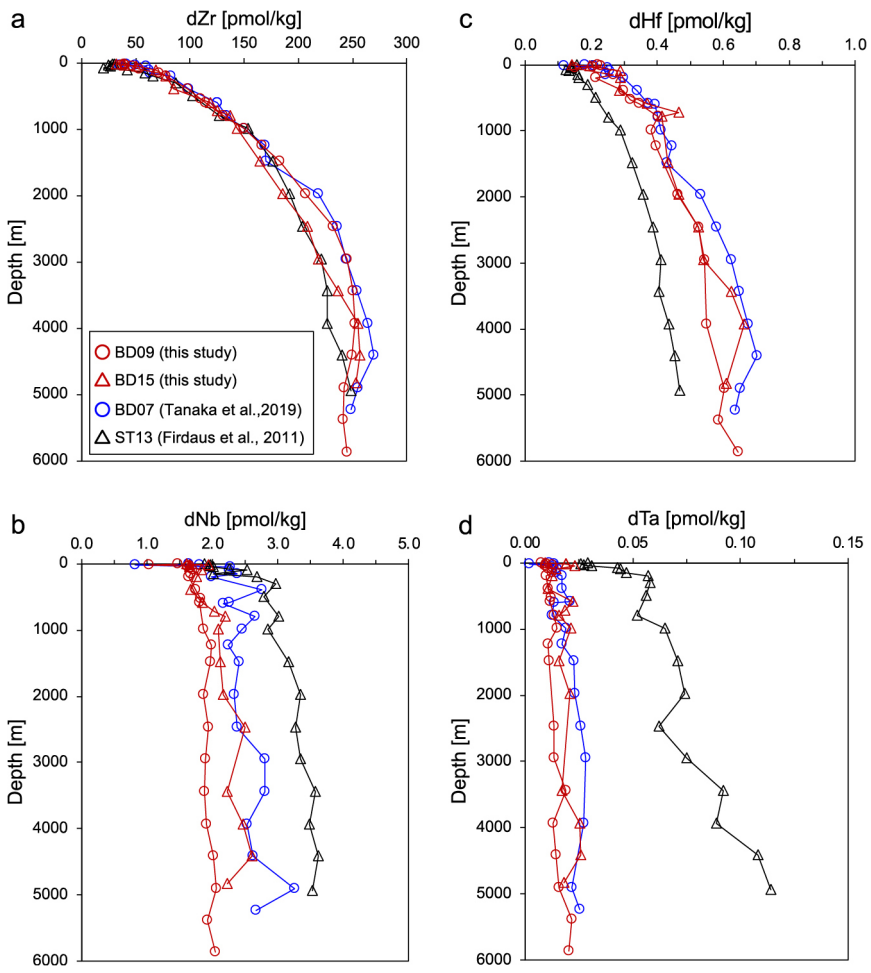

Fig. 5. Vertical profiles of (a) dZr, (b) dNb, (c) dHf, and (d) dTa at stations BD09 (red circles; 47.000 °N, 170.583 °E; this study), BD15 (red triangles; 50.834 °N, 160.000 °W; this study), BD07 (red circles; 47.000 °N, 160.086 °E; Tanaka *et al.*, 2019), and ST13 (black triangles; 50.005 °N, 159.983 °W; Firdaus *et al.*, 2011).

materials, which did not contain HF. Thus, Ta in the standard solutions may be adsorbed on the bottle, resulting in a systematically high value in calibration in the previous study (Firdaus *et al.*, 2011). Based on the above discussion, we believe that the data presented in this study are more accurate than the previous data (**Table 1**).

Relationship between the metals and $Si(OH)_4$

The concentrations of dZr and dHf in the subarctic North Pacific increased from surface water to deep water (**Fig. 3**), suggesting the influence of biogeochemical cycling on dZr and dHf distribution. Therefore, concentrations of the four elements in the North Pacific are compared to those of $Si(OH)_4$ (**Fig. 6**). The dZr and dHf showed strong correlations with $Si(OH)_4$ from the surface to a depth of 1500 m (dZr: $R^2 = 0.94$, dHf: $R^2 = 0.81$), while they increased independent of $Si(OH)_4$ in deep water. Such features have been reported in the literature (Godfrey *et al.*, 1996; McKelvey and Orians, 1993; Stichel *et al.*, 2012). The increase of dZr and dHf below 1500 m in depth indicates bottom sources of dZr and dHf. In contrast, the concentrations of dNb and dTa have small variations across the depth, showing no correlation with $Si(OH)_4$.

Fractionation of Zr/Hf and Nb/Ta in natural waters

The dZr/dHf mole ratio in surface water (0–200 m depths) was 260 ± 53 ($n = 20$), while that in deep water below 2000 m depth was 414 ± 24 ($n = 25$) (**Fig. 7**). The dNb/dTa mole ratio was 146 ± 48 ($n = 75$), showing little change from surface water to deep water. Although the dZr/dHf ratio in this study is comparable with that reported in our previous papers (Firdaus *et al.*, 2008, 2011), the dNb/dTa ratio in this study is 4–7 times higher than that reported in our previous papers (Firdaus *et al.*, 2008, 2011). The mole ratios of Zr/Hf and Nb/Ta in Ferromanganese (Fe-Mn) crusts collected from the Pacific Ocean (8 °S–15 °N, 177 °E–169 °W, depth 1400–2600 m) have been reported to be 145–190 and 105–177, respectively (Schmidt *et al.*, 2014). The Zr/Hf mole ratio in seawater below 2000 m in depth was higher than that in Fe-Mn crusts, suggesting that dHf is preferentially

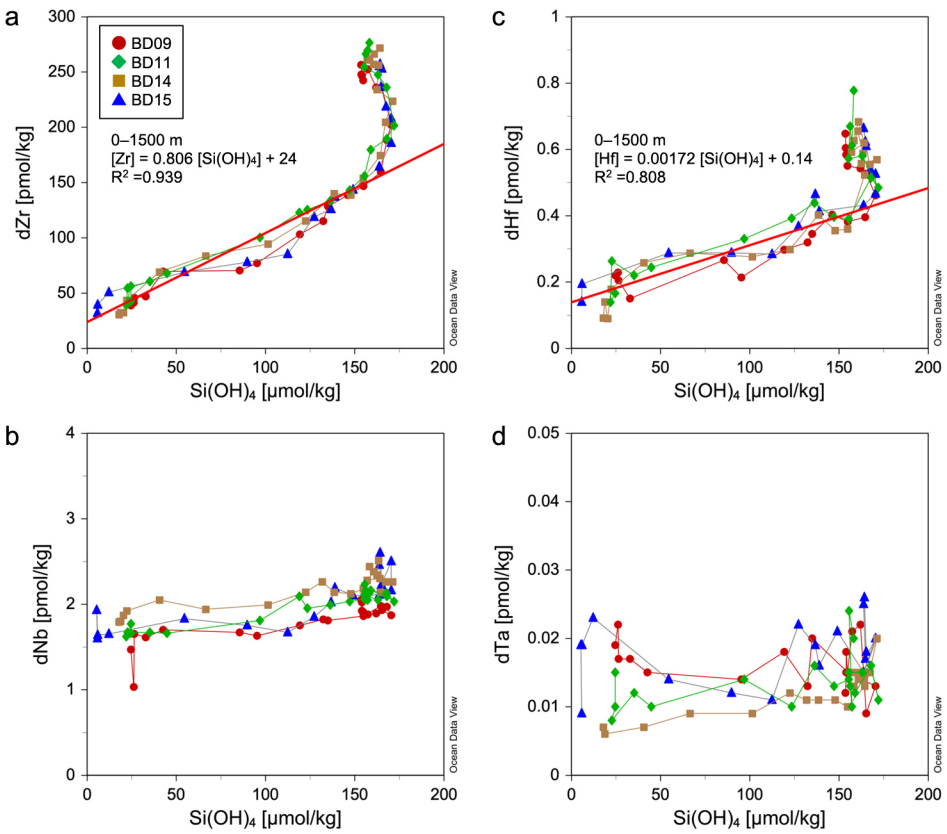

Fig. 6. Plots of (a) dZr, (b) dNb, (c) dHf, and (d) dTa versus $Si(OH)_4$ at stations BD09, BD11, BD14, and BD15. The red lines show the linear relationship between dissolved metals and $Si(OH)_4$ in a depth range of 0–1500 m.

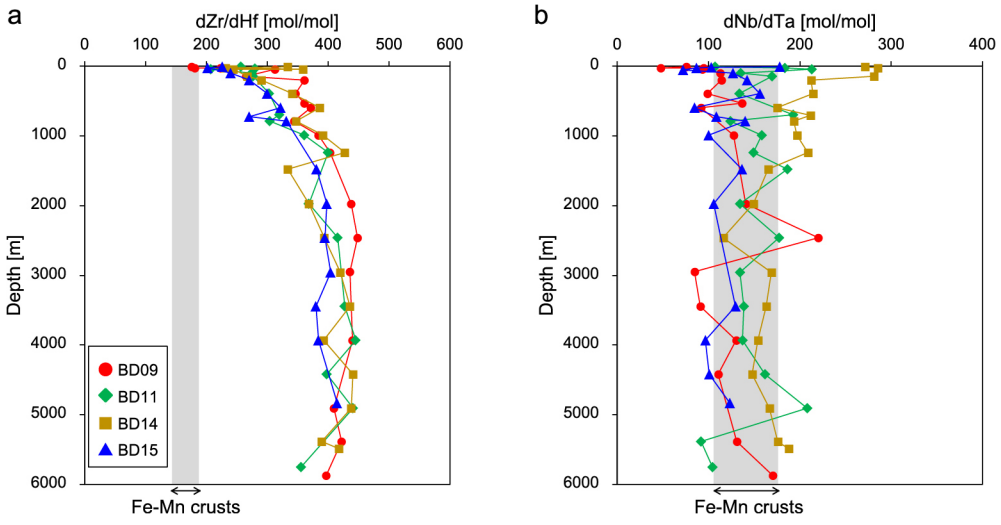

Fig. 7. Vertical profiles of (a) dZr/dHf mole ratio and (b) dNb/dTa mole ratio at stations BD09 (red circles), BD11 (green diamonds), BD14 (yellow squares), and BD15 (blue triangles). The gray columns show the mole ratio ranges of Zr/Hf and Nb/Ta in the surface layers (<1 mm from the surface) of Fe-Mn crusts from the Pacific Ocean (Schmidt *et al.*, 2014).

adsorbed on Fe-Mn crusts compared to dZr (Schmidt *et al.*, 2014). In contrast, the Nb/Ta ratio in deep seawater was equivalent to that in Fe-Mn crusts, suggesting that dNb and dTa are not fractionated when adsorbed on Fe-Mn crusts.

The dZr/dHf and dNb/dTa mole ratios of natural waters in this study are compared to Zr/Hf and Nb/Ta mole ratios in Fe-Mn crusts from the Pacific Ocean (Schmidt *et al.*, 2014) and continental crust (Rudnick and Gao, 2003) (**Fig. 8**). The dZr/dHf ratio in river water

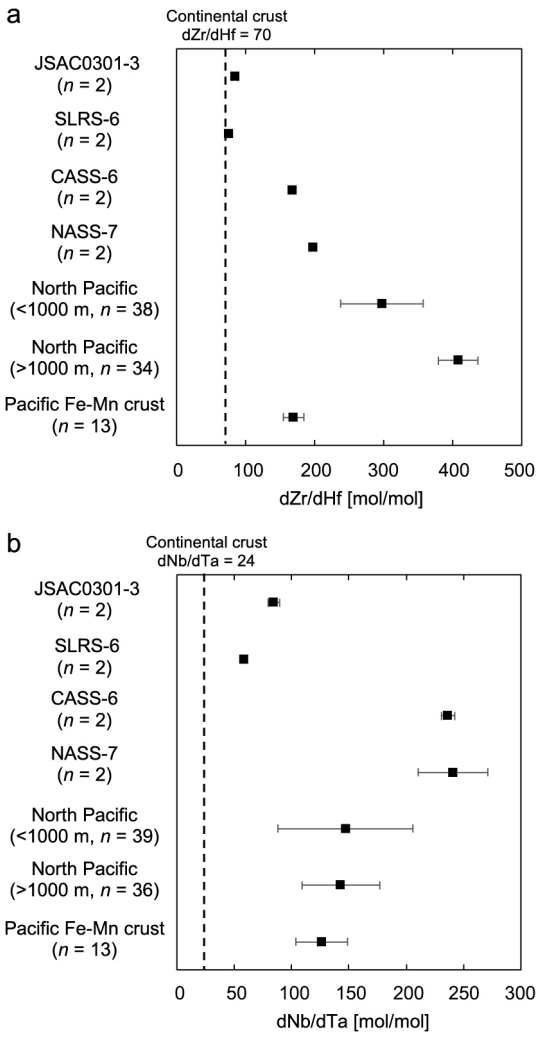

Fig. 8. (a) dZr/dHf mole ratio (mean ± sd) and (b) dNb/dTa mole ratio in river water (JSAC0301-3, SLRS-6; this study), coastal seawater (CASS-6, NASS-7; this study), the North Pacific Ocean seawater (this study). The dashed lines show mole ratios of Zr/Hf and Nb/Ta in the continental crust (Rudnick and Gao, 2003). The mole ratios of Zr/Hf and Nb/Ta in the surface layers (<1 mm from the surface) of Fe-Mn crusts collected from the Pacific Ocean (Schmidt *et al.*, 2014) are also shown for comparison.

(JSAC0301-3, SLRS-6) was close to the Zr/Hf ratio of the continental crust. Therefore, significant fractionation of Zr and Hf does not occur during weathering (Godfrey *et al.*, 2008). The dZr/dHf mole ratio increases in the order: river water < coastal seawater < open ocean seawater. This increase may reflect the preferential removal of dHf by particles compared to dZr (Censi *et al.*, 2018; Sasmaz *et al.*, 2021). It has been proposed that the inflow of colloidal Zr and Hf from rivers to the ocean is extremely low because they are removed from the river water during estuarine mixing (Bau and Koschinsky, 2006). The Zr/Hf ratio in Fe-Mn crusts was nearly half of dZr/dHf ratio in seawater, indicating preferential incorporation of dHf into Fe-Mn crusts.

The dNb/dTa ratio in river water was higher than Nb/Ta ratio of the continental crust, suggesting that Nb is preferentially dissolved during weathering. In natural waters, the dNb/dTa ratio increased in the order: river water < open ocean seawater < coastal seawater, suggesting multiple sources and sinks for dNb and dTa. Further comprehensive data are needed to clarify sources and sinks for dNb and dTa. The Nb/Ta ratio in Fe-Mn crusts was within a range of dNb/dTa ratio in seawater, indicating insignificant fractionation between dNb and dTa during their incorporation into Fe-Mn crusts.

Conclusions

In this study, we have improved our analytical method using the TSK-8HQ resin through optimization of the conditions for preconcentration, elution, evaporation, and redissolution. The procedural blank for dZr, dNb, dHf, and dTa were 2.0 ± 0.9, 0.05 ± 0.03, 0.03 ± 0.02, and 0.006 ± 0.002 pmol/kg (mean ± sd, n = 30), respectively. Recovery of Zr, Nb, Hf, and Ta from a seawater sample was 100 ± 4% for Zr, 100 ± 4% for Nb, 101 ± 3% for Hf, and 103 ± 6% for Ta (n = 10). The concentrations of dZr, dNb, dHf, and dTa in reference materials of seawater and river water were close to those of the selected previous studies. Therefore, our analytical method is useful for accurate determination of Zr, Nb, Hf, and Ta in seawater.

The concentration range of dZr, dNb, dHf, and dTa in the subarctic North Pacific Ocean was 30–276, 1.0–2.6, 0.09–0.78, and 0.006–0.026 pmol/kg, respectively. There was little difference between tdM and dM concentrations for each element, indicating lpM is a negligible fraction. The vertical profiles of dZr, dNb, and dHf in this study were similar to those of the previous studies (Firdaus *et al.*, 2011; Tanaka *et al.*, 2019). The vertical profile of dTa in this study was similar to that of our previous study (Tanaka *et al.*, 2019), while the dTa concentration was approximately one-fifth of that in the previous study (Firdaus *et al.*, 2011). The dTa concentration in the previous study (Firdaus *et al.*, 2011) may have affected by a systematic error. To the best of our knowledge, this study reports the east-west cross-sectional distribution of the four elements in the subarctic North Pacific Ocean for the first time.

Acknowledgments The authors thank the crew, technicians, scientists, and students onboard the KH12-4 cruise for their assistance with sampling and routine analysis of seawater. This research was supported by the establishment of university fellowships towards the creation of science technology innovation, Grant Number JPMJFS2123, to RU from the Japan Science and Technology Agency and by the Japan Society for the Promotion of Science (JSPS) KAKENHI grants (24241004, 15H01727, and 19H01148 to YS). The raw data of this study can be found in the supplementary file. We would like to thank Editage (www.editage.jp) for the English language editing.

References

Babechuk, M. G., O'Sullivan, E. M., McKenna, C. A., Rosca, C., Nagler, T. F., Schoenberg, R. and Kamber, B. S. (2020) Ultra-trace element characterization of the Central Ottawa River Basin using a rapid, flexible, and low-volume ICP-MS method. *Aquat. Geochem.* **26**, 327–374. https://doi.org/10.1007/s10498-020-09376-w

Bau, M. and Koschinsky, A. (2006) Hafnium and neodymium isotopes in seawater and in ferromanganese crusts: The "element perspective". *Earth Planet. Sci. Lett.* **241**, 952–961. https://doi.org/10.1016/j.epsl.2005.09.067

Bayon, G., Birot, D., Bollinger, C. and Barrat, J. A. (2011) Multi-element determination of trace elements in natural water reference materials by ICP-SFMS after Tm addition and iron co-precipitation. *Geostand. Geoanal. Res.* **35**, 145–153. https://doi.org/10.1111/j.1751-908X.2010.00064.x

Byrne, R. H. (2002) Inorganic speciation of dissolved elements in seawater: The influence of pH on concentration ratios. *Geochem. Trans.* **3**, 11–16. https://doi.org/10.1186/1467-4866-3-11

Censi, P., Sposito, F., Inguaggiato, C., Zuddas, P., Inguaggiato, S. and Venturi, M. (2018) Zr, Hf and REE distribution in river water under different ionic strength conditions. *Sci. Total Environ.* **645**, 837–853. https://doi.org/10.1016/j.scitotenv.2018.07.081

Firdaus, M. L., Norisuye, K., Sato, T., Urushihara, S., Nakagawa, Y., Umetani, S. and Sohrin, Y. (2007) Preconcentration of Zr, Hf, Nb, Ta and W in seawater using solid-phase extraction on TSK-8-hydroxyquinoline resin and determination by inductively coupled plasma-mass spectrometry. *Anal. Chim. Acta.* **583**, 296–302. https://doi.org/10.1016/j.aca.2006.10.033

Firdaus, M. L., Norisuye, K., Nakagawa, Y., Nakatsuka, S. and Sohrin, Y. (2008) Dissolved and labile particulate Zr, Hf, Nb, Ta, Mo and W in the western North Pacific Ocean. *J. Oceanogr.* **64**, 247–257. https://doi.org/10.1007/s10872-008-0019-z

Firdaus, M. L., Minami, T., Norisuye, K. and Sohrin, Y. (2011) Strong elemental fractionation of Zr-Hf and Nb-Ta across the Pacific Ocean. *Nat. Geosci.* **4**, 227–230. https://doi.org/10.1038/ngeo1114

Firdaus, M. L., Mashio, A. S., Obata, H., McAlister, J. A. and Orians, K. J. (2018) Distribution of zirconium, hafnium, niobium and tantalum in the North Atlantic Ocean, northeastern Indian Ocean and its adjacent seas. *Deep-Sea Res. I: Oceanogr. Res. Pap.* **140**, 128–135. https://doi.org/10.1016/j.dsr.2018.08.008

Godfrey, L. V., White, W. M. and Salters, V. J. M. (1996) Dissolved zirconium and hafnium distributions across a shelf break in the northeastern Atlantic Ocean. *Geochim. Cosmochim. Acta.* **60**, 3995–4006. https://doi.org/10.1016/s0016-7037(96)00246-3

Godfrey, L. V., Field, M. P. and Sherrell, R. M. (2008) Estuarine distributions of Zr, Hf, and Ag in the Hudson River and the implications for their continental and anthropogenic sources to seawater. *Geochem. Geophys.* **9**, Q12007. https://doi.org/10.1029/2008gc002123

Godfrey, L. V., Zimmermann, B., Lee, D.-C., King, R. L., Vervoort, J. D., Sherrell, R. M. and Halliday, A. N. (2009) Hafnium and neodymium isotope variations in NE Atlantic seawater. *Geochem. Geophys.* **10**, Q08015. https://doi.org/10.1029/2009GC002508

McKelvey, B. A. and Orians, K. J. (1993) Dissolved zirconium in the north Pacific Ocean. *Geochim. Cosmochim. Acta.* **57**, 3801–3805. https://doi.org/10.1016/0016-7037(93)90157-R

McKelvey, B. A. and Orians, K. J. (1998) The determination of dissolved zirconium and hafnium from seawater using isotope dilution inductively coupled plasma mass spectrometry. *Mar. Chem.* **60**, 245–255. https://doi.org/10.1016/s0304-4203(97)00101-1

Nakagawa, Y., Firdaus, M. L., Norisuye, K., Sohrin, Y., Irisawa, K. and Hirata, T. (2008) Precise isotopic analysis of Mo in seawater using multiple collector-inductively coupled mass spectrometry coupled with a chelating resin column preconcentration method. *Anal. Chem.* **80**, 9213–9219. https://doi.org/10.1021/ac801383t

Poehle, S. and Koschinsky, A. (2017) Depth distribution of Zr and Nb in seawater: The potential role of colloids or organic complexation to explain non-scavenging-type behavior. *Mar. Chem.* **188**, 18–32. https://doi.org/10.1016/j.marchem.2016.12.001

Poehle, S., Schmidt, K. and Koschinsky, A. (2015) Determination of Ti, Zr, Nb, V, W and Mo in seawater by a new online-preconcentration method and subsequent ICP–MS analysis. *Deep-Sea Res. I: Oceanogr. Res. Pap.* **98**, 83–93. https://doi.org/10.1016/j.dsr.2014.11.014

Rahlf, P., Laukert, G., Hathorne, E. C., Vieira, L. H. and Frank, M. (2021) Dissolved neodymium and hafnium isotopes and rare earth elements in the Congo River Plume: Tracing and quantifying continental inputs into the southeast Atlantic. *Geochim. Cosmochim. Acta.* **294**, 192–214. https://doi.org/10.1016/j.gca.2020.11.017

Raso, M., Censi, P. and Saiano, F. (2013) Simultaneous determinations of zirconium, hafnium, yttrium and lanthanides in seawater according to a co-precipitation technique onto iron-hydroxide. *Talanta.* **116**, 1085–1090. https://doi.org/10.1016/j.talanta.2013.08.019

Rickli, J., Frank, M. and Halliday, A. N. (2009) The hafnium–neodymium isotopic composition of Atlantic seawater. *Earth Planet. Sci. Lett.* **280**, 118–127. https://doi.org/10.1016/j.epsl.2009.01.026

Rickli, J., Gutjahr, M., Vance, D., Fischer-Gödde, M., Hillenbrand, C.-D. and Kuhn, G. (2014) Neodymium and hafnium boundary contributions to seawater along the West Antarctic continental margin. *Earth Planet. Sci. Lett.* **394**, 99–110. https://doi.org/10.1016/j.epsl.2014.03.008

Rudnick, R. L. and Gao, S. (2003) Composition of the continental crust. *Treatise on Geochemistry* Volume 3: The Crust (Holland, H. D. and Turekian, K. K., eds.), 1–64, Elsevier Science. https://doi.org/10.1016/B0-08-043751-6/03016-4

Sasmaz, A., Zuddas, P., Cangemi, M., Piazzese, D., Ozek, G., Venturi, M. and Censi, P. (2021) Zirconium and hafnium fractionation and distribution of Rare Earth Elements in neutral–alkaline waters: Case study of Lake Van hydrothermal system, Turkey. *J. Geochem. Explor.* **226**, 106784. https://doi.org/10.1016/j.gexplo.2021.106784

Schmidt, K., Bau, M., Hein, J. R. and Koschinsky, A. (2014) Fractionation of the geochemical twins Zr-Hf and Nb-Ta during scavenging from seawater by hydrogenetic ferromanganese crusts. *Geochim. Cosmochim. Acta.* **140**, 468–487. https://doi.org/10.1016/j.gca.2014.05.036

Sohrin, Y. and Bruland, K. W. (2011) Global status of trace elements in the ocean. *TrAC, Trends Anal. Chem.* **30**, 1291–1307. https://doi.org/10.1016/j.trac.2011.03.006

Sohrin, Y., Fujishima, Y., Ueda, K., Akiyama, S., Mori, K., Hasegawa, H. and Matsui, M. (1998) Dissolved niobium and tantalum in the North Pacific. *Geophys. Res. Lett.* **25**, 999–1002. https://doi.org/10.1029/98GL00646

Stichel, T., Frank, M., Rickli, J. and Haley, B. A. (2012) The hafnium and neodymium isotope composition of seawater in the Atlantic sector of the Southern Ocean. *Earth Planet. Sci. Lett.* **317–318**, 282–294. https://doi.org/10.1016/j.epsl.2011.11.025

Sun, S. and Li, J. (2015) Determination of Zr, Nb, Mo, Sn, Hf, Ta, and W in seawater by N-benzoyl-N-phenylhydroxylamine extraction

chromatographic resin and inductively coupled plasma-mass spectrometry. *Microchem. J.* **119**, 102–107. https://doi.org/10.1016/j.microc.2014.11.006

Tanaka, Y., Tsujisaka, M., Zheng, L., Takano, S. and Sohrin, Y. (2019) Application of NOBIAS Chelate-PA 1 resin to the determination of zirconium, niobium, hafnium, and tantalum in seawater. *Anal. Sci.* **35**, 1015–1020. https://doi.org/10.2116/analsci.19P069

Yeghicheyan, D., Aubert, D., Bouhnik-Le Coz, M., Chmeleff, J., Delpoux, S., Djouraev, I., Granier, G., Lacan, F., Piro, J.-L. Rousseau, T., Cloquet, C., Marquet, A., Menniti, C., Pradoux, C., Freydier, R., Vieira da Silva-Filho, E. and Suchorski, K. (2019) A new interlaboratory characterisation of silicon, rare earth elements and twenty-two other trace element concentrations in the natural river water certified reference material SLRS-6 (NRC-CNRC). *Geostand. Geoanal. Res.* **43**, 475–496. https://doi.org/10.1111/ggr.12268

Zheng, L., Minami, T., Konagaya, W., Chan, C.-Y., Tsujisaka, M., Takano, S., Norisuye, K. and Sohrin, Y. (2019) Distinct basin-scale-distributions of aluminum, manganese, cobalt, and lead in the North Pacific Ocean. *Geochim. Cosmochim. Acta.* **254**, 102–121. https://doi.org/10.1016/j.gca.2019.03.038

Supplementary Materials

https://www.jstage.jst.go.jp/article/geochemj/57/5/57_GJ23013/_article

- Supplementary Figs. 1, 2
- Supplementary Tables 1–5